Acta Pharmacologica Sinica (2009) 30: 1359–1368
 1671-4083/09 $32.00
www.nature.com/aps

Original Article

LGH00031, a novel ortho-quinonoid inhibitor of cell division cycle 25B, inhibits human cancer cells via ROS generation

Yu-bo ZHOU#, Xu FENG#, Li-na WANG, Jun-qing DU, Yue-yang ZHOU, Hai-ping YU, Yi ZANG, Jing-ya LI, Jia LI*

National Center for Drug Screening, Shanghai Institute of Materia Medica, Chinese Academy of Sciences, Shanghai 201203, China

Aim: To discover novel cell division cycle 25 (CDC25) B inhibitors and elucidate the mechanisms of inhibition in cancer cells.
Methods: Cell growth inhibition was detected by MTT assay, the cell cycle was analyzed by flow cytometry, and protein expression and phosphorylation was examined by Western blot analysis.
Results: LGH00031 inhibited CDC25B irreversibly *in vitro* in a dose-dependent manner, and impaired the proliferation of tumor cell lines. In synchronized HeLa cells, LGH00031 delayed the cell cycle progression at the G_2/M phase. LGH00031 increased cyclin-dependent kinase 1 (CDK1) tyrosine 15 phosphorylation and cyclin B1 protein level. The activity of LGH00031 against CDC25B *in vitro* relied on the existence of 1,4-dithiothreitol (DTT) or dihydrolipoic acid and oxygen. The oxygen free radical scavenger catalase and superoxide dismutase reduced the inactivation of CDC25 by LGH00031, confirming that reactive oxygen species (ROS) mediate the inactivation process *in vitro*. LGH00031 accelerated cellular ROS production in a dose-dependent manner, and *N*-acetyl cysteine (NAC) markedly decreased the ROS production induced by LGH00031. Correspondingly, the LGH00031-induced decrease in cell viability and cell cycle arrest, cyclin B1 protein level, and phosphorylation of CDK1 tyrosine 15 were also rescued by NAC that decreased ROS production.
Conclusion: The activity of LGH00031 at the molecular and cellular level is mediated by ROS.

Keywords: LGH00031; ortho-quinone; CDC25B; irreversible inhibitor; ROS

Acta Pharmacologica Sinica (2009) 30: 1359–1368; doi: 10.1038/aps.2009.131

Introduction

CDC25, a subfamily of dual-specificity protein tyrosine phosphatases, which includes CDC25A, B, and C homologues, plays a pivotal role in the regulation of the cell cycle[1]. CDC25 phosphatases, particularly the CDC25A and CDC25B isoforms, are overexpressed in primary tissue samples from various human cancers, and this overexpression is strongly associated with tumor aggressiveness and poor prognosis[2–5]. The coexpression of CDC25A or CDC25B cooperates with either oncogenic HRAS or the loss of RB1 to transform mouse embryonic fibroblasts, resulting in the capability of forming high-grade tumors *in vivo*[6]. In addition, overexpression of CDC25B in the mammary glands of mice increases the proliferation of mammary epithelial cells and hyperplasia, which induces tumor growth when also challenged with the carcinogen 9,10-dimethyl-1,2-benzanthracene[7, 8]. Conversely, downregulating the expression of CDC25B by microinjecting antibodies against CDC25B causes G2 arrest, whereas RNA interference against CDC25A causes G1 arrest and significant inhibition of cancer cell invasion[9, 10]. These findings in turn make CDC25 A and B ideal targets for a new anticancer therapy.

The identified CDC25 inhibitory compounds, which inhibit all three CDC25 isoforms, belong to various groups including phosphate surrogates, electrophilic entities, and quinonoids[11]. Phosphate surrogates mimic the phosphate of the natural substrate of enzymes and locates at the phosphate-binding pocket, which prevents the entry of the substrate, such as dysidiolide analogues[12, 13]. At physiological pH, the active-site cysteine exists as a thiolate with a pK_a of ~5.9 (in comparison with ~8.0 for free cysteine). Thus, electrophilic entities such as PM-20 might easily attack the cysteine or one of the vicinal serines, leading to the covalent modification of the enzyme[14]. The most potent CDC25 phosphatase inhibitors reported to date include the para- and ortho-quinonoids. The para-quinonoid probably acts through the irreversible oxidation of the cysteine residue in the catalytic domain (CX_5R) of CDC25 phosphatases into a sulfonic acid (Cys-SO_3^-), such as NSC 663284[15].

# These authors contributed equally to this work.
* To whom correspondence should be addressed.
E-mail jli@mail.shcnc.ac.cn
Received 2009-06-11 Accepted 2009-07-21

Only a few ortho-quinonoid compounds have been reported to be CDC25 inhibitors, and the mechanisms of action are still unclear. Ortho-quinonoid skeleton tanshinones, such as cryptotanshinones and miltirone analogues reported by our group, are moderate inhibitors of CDC25B with the half maximal inhibitory concentration (IC_{50}) of 3.2–24 μmol/L[16, 17]. Here we report on a novel ortho-quinonoid inhibitor of CDC25B, LGH00031, which has better activity against CDC25B and cancer cells. And the mechanism of inhibition was further studied.

Materials and methods

Materials and instruments

The plasmid pGEX–KG was a kind gift from Dr Kun-liang GUAN of the University of Michigan (Ann Arbor, MI, USA). The restriction enzymes and Ex *Taq* polymerase were purchased from TaKaRa (Dalian, China). Escherichia coli strain BL21–CodonPlus (DE3) was from Stratagene (La Jolla, CA, USA). GSTrap FF and HiPrep 26/10 desalting columns were obtained from Amersham Pharmacia Biotech (Uppsala, Sweden). Substrate *p*-nitrophenyl phosphate (pNPP) was from Calbiochem (San Diego, CA, USA). 2′,7′-dichlorofluorescein diacetate (H_2DCFDA), 1,4-dithiothreitol (DTT), 3-*O*-methylfluorescein phosphate (OMFP), dihydrolipoic acid, catalase from bovine liver (2000–5000 units/mg) and superoxide dismutase (SOD) from horseradish (3000 units/mg) were from Sigma Aldrich (St Louis, MO, USA). High-glucose Dulbecco's modified Eagle' medium (HG-DMEM), McCoy's 5A and F12 medium were from Invitrogen (Carlsbad, CA, USA). Fetal bovine serum (FBS) was purchased from Hyclone (Logan, UT, USA). 3-(4,5-dimethylthiazol-2-yl)-2, 5-diphenyltetrazoliom bromide (MTT), and propidium iodide were from Sigma. The antibodies for CDK1, Tyr15-p CDK1 and cyclin B1, anti-β-actin, horseradish peroxidase (HRP)-linked anti-mouse immunoglobulin (IgG) and anti-rabbit IgG were purchased from Cell Signal Technology (Danvers, MA, USA). The nitrocellulose membranes were from Amersham Biosciences (Piscataway, New Jersey, USA) and the enhanced chemiluminescence (ECL) reagents were from Calbiochem (San diego, CA, USA). Other solvents and reagents used in experiments were of analytical grade.

Polymerase chain reaction (PCR) was performed using GeneAmp PCR System2400 from PerkinElmer (Norwalk, CT, USA). Continuous kinetic monitoring of enzyme activity was performed on SPECTRAmax 340 or Flexstation^2-384 microplate reader (Molecular Devices, Sunnyvale, CA, USA) and controlled by the Softmax software. Liquid handling for random screening was carried out with a Biomek FX from Beckman Coulter (Fullerton, CA, USA) and HYTRA-96 semi-automated 96-channel pipettors from Robbins (Sunnyvale, CA, USA). Cell circle analysis was carried out with a FACSCalibur Cell Sorting System from BD Bioscience (Franklin Lakes, NJ, USA).

Construction, expression, and purification of the CDC25B catalytic domain

The cDNA of the CDC25B catalytic domain (1354−1923 nt according to gi11641416) was cloned into the pGEX–KG expression vector. The protein was expressed as a glutathione-*S*-transferase (GST) fusion protein in *Escherichia coli* BL21–CodonPlus (DE3) and purified with glutathione sepharose column as previously described[18].

CDC25B activity assay and kinetics study

The enzymatic activities of the CDC25B catalytic domain were determined by monitoring the dephosphorylation of OMFP. Dephosphorylation of OMFP generates product OMF, which was detected at a 485 nm excitation/530 nm emission. In a typical 100 μL assay mixture containing 50 mmol/L Tris-HCl, 50 mmol/L NaCl, pH 8.0, 5 μmol/L OMFP, 20 nmol/L recombinant CDC25B, 1% glycerin, 1 mmol/L DTT, in presence or absence of 2 μL inhibitor in dimethyl sulfoxide (DMSO), activities were continuously monitored and the initial rate of the dephosphorylation was determined using the early linear region of the enzymatic reaction kinetic curve. Continuous kinetic monitoring was performed in clear 96-well plates (Corning, Lowell, MA).

To obtain an estimate of the observed inactivation rate (k_{obs}) at a specific concentration of inhibitor, CDC25B was preincubated with compound in various times prior to initiation of reaction with OMFP. Data from such an experiment can be fit to the following equation: $V_t = V_i \exp(-k_{obs}\, t)$ (24) where V_t is the measured steady state velocity after preincubation time t, and V_i is the steady state velocity when preincubation time is zero. By these methods we can obtain an estimate of k_{obs} at varying concentrations of inhibitor, and then use the results to yield an apparent inactivation rate constant (k_{obs}/I) to quantify the effectiveness of the inhibitor.

To create oxygen-free conditions, CDC25B in assay buffer (contained 1 mmol/L DTT) was exchanged with helium gas for three cycles in a rubber septum-sealed round-bottom flask. And then 10 times concentrated inhibitor in DMSO was injected into the mixture under nitrogen. After incubation in indicated time, 22 μL of the mixture was taken out by syringe and the residual activity was monitored.

Selectivity of LGH00031 on other PTPase family members

CDC25A and some other PTPase family members, such as Src homology domain 2 (SH2)-containing tyrosine phosphatase-1 (SHP1), leukocyte antigen-related phosphatase (LAR D1 D2), Jun amino-terminal kinase (JNK) stimulatory phosphatase-1 (JSP-1), CD45, protein tyrosine phosphatase 1B (PTP1B) and vaccinia virus VH-1-related dual-specific protein phosphatase (VHR), were prepared for evaluating the selectivity of LGH00031 on those members. CDC25A (1373–1939 nt according to gi33873622), PRL-3 (335-856 nt according to gi14589855), SHP1 (244–570 according to BC002523), LAR D1 D2 (4192-6061 according to gi109633040), JSP-1 (443-991 according to BC022847), CD45 (1698-3791 according to gi115385976), PTP1B (91–1053 according to gi190741), and VHR (56–613 according to BC002682) cDNA were cloned into pGEX-KG. GST–PTPase were overexpressed as GST-fusion proteins in *Escherichia coli* BL21-CondenPlus (DE3) and purified by affinity chromatogra-

phy. Assays for the other PTPase were performed at the optimal pH for individual enzyme activity. These enzymes and inhibitors were preincubated for 10 min at 4 °C, and the assays were initiated by adding substrates. Assays performed for CDC25B, JSP1, VHR and SHP1 were using OMFP as substrate. And that for LARD1D2, PTP1B, CD45 were pNPP, which can generate pNP after dephosphorylation. The pNP was monitored at an absorbance of 405 nm.

ROS production determination

ROS production was monitored with H_2DCFDA reagent. The 100 μL assay system contained 10 μmol/L H_2DCFDA, 2 μL inhibitor and reducing agents (as indicated in the text) in CDC25B assay buffer. Oxidation of the probe was detected in clear 96-well plate by monitoring the increase in fluorescence intensity at 525 nm emission after 490 nm excitation (top readout). The fluorescence intensity after reaction for 60 min (except continuous kinetic monitoring) was used to quantify the ROS signal.

In cellular ROS assay, H_2DCFDA was added directly to the cell culture at a final concentration of 10 μmol/L and incubated for 30 min at 37 °C. The cells were washed three times with PBS, and the relative levels of cytosolic ROS were detected by FACS analysis.

Cell culture

HeLa, HCT116 and A549 cells were kept at logarithmic growth in 5% CO_2 at 37 °C with HG-DMEM, McCoy's 5A and F12 medium, respectively, supplemented with 10% FBS and 100 units/mL each of penicillin G and streptomycin.

Cell proliferation assay

Tumor cells were seeded onto a 96-well plate at a concentration of 2000 cells/well and incubated at 37 °C in 5% CO_2 for 24 h. A range of concentrations of the test compounds were added and the plate was incubated at 37 °C for 72 h before 40 μL MTT (5 mg/mL)/well was added. After 3 h incubation, the medium was removed and 100 μL DMSO was added to each well. The absorbance was measured on SpectraMax 340 microplate reader at 550 nm with a reference at 690 nm. The optical density of the result in MTT assay was directly proportional to the number of viable cells.

Flow cytometric analysis

Exponentially growing HeLa cells (1.5×10^5 cells/well) were treated with LGH00031 (0, 1, 2, 5, and 10 μmol/L) in 6-well plates at 37 °C for 12 h. The cells were then harvested by trypsin digestion, washed twice with cold PBS suspended in cold 70% ethanol, and incubated at 4 °C overnight. The cells were stained with a PBS solution containing 20 μg/mL propidium iodide and 200 μg/mL RNase A and analyzed by flow cytometry. The experiment was repeated at least 3 independent times. Cells treated with the vehicle, 1% DMSO.

Western blot

Cells were rinsed twice with PBS and then lysed with 1×SDS loading buffer. The samples were analyzed by 10% SDS-PAGE gels and transferred to nitrocellular membranes. The membranes were blocked for 1 h with 5% (*w/v*) bovine serum albumin and incubated with the primary antibodies overnight at 4 °C and the secondary antibodies for 1 h at room temperature. Antigen-antibody complexes were detected with the ECL kit. The densitometric analysis of band intensity was performed using the Quantity One 1-D Analysis Software (Bio-Rad Laboratories, Inc, CA, USA), and was normalized with β-actin intensity.

Results

LGH00031 inhibited CDC25B irreversibly *in vitro*

To find novel small-molecule inhibitors, an high throughput screening (HTS) with recombinant CDC25B was developed[18]. After determining the hit validation and dose-response curve, the compound LGH00031 with a novel structure (Figure 1A, chemical name: 8-bromo-2-(isopropylamino-methyl)-3-methyl-4,5-dioxo-4,5-dihydro-3*H*-benzo[e] indole-1-carboxylic acid ethyl ester) was discovered to potently inhibit CDC25B in a dose- and time-dependent manner with an IC_{50} of 0.97 μmol/L (Figure 1B).

To identify the inhibition pattern of LGH00031, dialysis was used to study the reversibility of LGH00031 inhibition. As shown in Figure 1C, after dialysis for 2, 4, 6, and even 25 h, the activity of CDC25B was not rescued from the inhibition by LGH00031, indicating that the compound inhibited CDC25B irreversibly.

We then observed the inactivation rate (k_{obs}) at a different concentration of inhibitor. The relationship between k_{obs} and the concentration of the inhibitor is shown in Figure 1D. The observed rate of inactivation increased nearly linearly with increased LGH00031 concentration, yielding an apparent inactivation rate constant (k_{obs}/I) of 7579±647 $s^{-1}\cdot(mol/L)^{-1}$ within the linear response zone.

The selectivity of the compound on protein tyrosine phosphatases (PTPases) was also evaluated. The IC_{50} values of the effect of LGH00031 on CDC25A, CDC25B, SHP1, LARD1D2, JSP1, CD45, PTP1B, and VHR were measured in parallel. As shown in Table 1, LGH00031 had a more potent selectivity on the CDC25s than on the other PTPase family members, whereas there was no difference between the subfamily of CDC25B and CDC25A (IC_{50}: 1.25±0.02 μmol/L).

LGH00031 inhibited cell proliferation and induced cell cycle arrest

A549, HeLa, and HCT116 cells were used to investigate the effect of LGH00031 on the proliferation of cancer cells. Cells were seeded at 2000 cells per well in a 96-well microplate. After 24 h, cells were treated with the indicated concentration of LGH00031 for 72 h, using 1% dimethyl sulfoxide (DMSO) as a negative control. The viability of cells was evaluated with the MTT method. As shown in Figure 2A, LGH00031 markedly inhibited the proliferation of A549 cells (IC_{50}: 0.328±0.015 μmol/L), HeLa cells (IC_{50}: 0.290±0.012 μmol/L), and HCT116 cells (IC_{50}: 0.143±0.003 μmol/L).

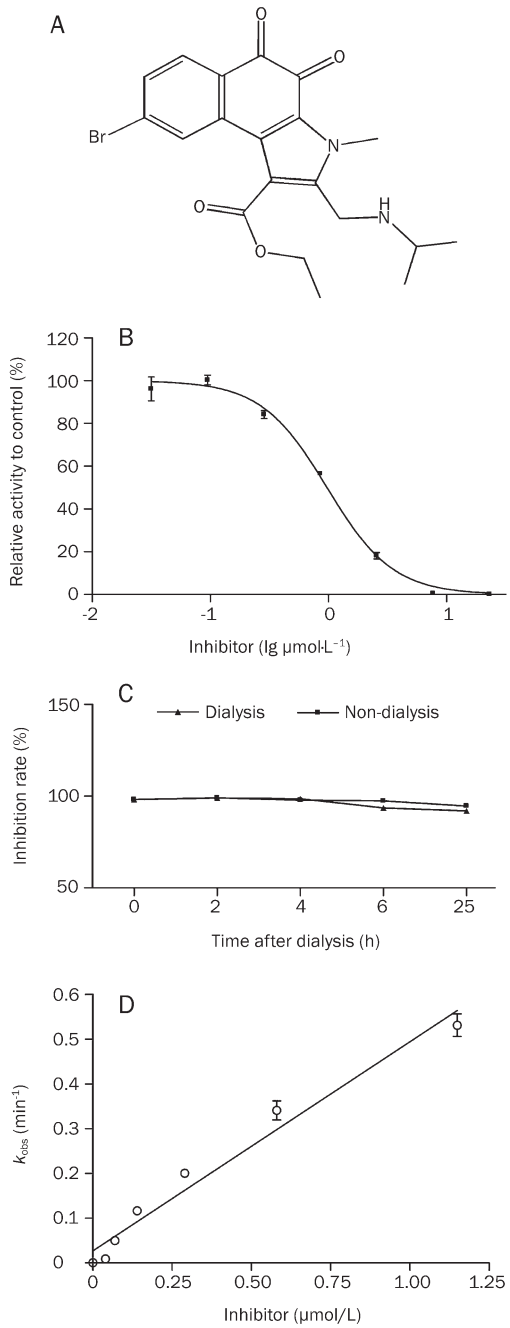

Figure 1. LGH00031 inhibited CDC25B irreversibly *in vitro*. (A) Chemical structure of LGH00031. (B) Dose–dependent inhibition of CDC25B by LGH00031. (C) Irreversible inhibition of LGH00031 against CDC25B. The enzyme-inhibitor complex including 0.2 μmol/L CDC25B and 34.6 μmol/L LGH00031 was dialyzed against 5000-fold of the assay buffer for the indicated period of time. At the end of each dialysis, CDC25B activity was determined in a typical assay. (D) The relationship between k_{obs} and the concentration of the inhibitor.

Because of the prominent role of CDC25B in controlling mitosis, HeLa cells were used to investigate the effect of LGH00031 on cell cycle progress. HeLa cells (1.5×10^5) were plated in a six-well plate. Cells were synchronized in the late G_1 phase by double thymidine block and released for 8 h with about 88% of the population displaying G_2/M phase DNA content. The synchronized cells were then treated with the indicated concentration of LGH00031 and nocodazole or 1% DMSO for 10 h. The cells treated with increasing concentrations of LGH00031 were blocked at the G_2/M phase in a dose-dependent manner, whereas the DMSO-treated control cells had completed mitosis within 10 h and had entered the following cell cycle (Figure 2B). Such results indicate that LGH00031 can target and delay the cell cycle progression at the G_2/M phase.

Table 1. IC_{50} values (μmol/L, mean±SEM, n=3) of LGH00031 against recombinant human CDC25B, CDC25A, VHR, JSP1, CD45, PTP1B, LARD1D2, and SHP1.

PTPs	IC_{50} (μmol/L)
CDC25B	0.97±0.05
CDC25A	1.25±0.02
SHP1	15.09±2.46
LARD1D2	36.08±14.82
JSP1	3.58±0.22
CD45	10.72±1.90
PTP1B	6.03±0.89
VHR	4.88±0.34

LGH00031 inhibited CDK1 dephosphorylation and delayed the entry into mitosis

CDC25B is known to play an essential role in the control of CDK activity during mitosis. We used Western blot analysis to examine the phosphorylation of CDK1 at tyrosine 15. HeLa cells were synchronized at the G_2/M phase as described above and treated with LGH00031 or 1% DMSO. After 4 h, cells were harvested for Western blot analysis. As shown in Figure 2C and 2D, the effect of LGH00031 on the phosphorylation of CDK1 was concentration-dependent. The expression level of cyclin B1 in the same experiment was also examined by Western blot analysis. Cyclin B1 protein accumulated with increasing concentration of LGH00031, indicating that the cells were prevented from entering mitosis by inhibition of CDC25.

The activity of LGH00031 against CDC25B *in vitro* relied on DTT or dihydrolipoic acid and oxygen

It has been reported that quinonoid compounds need thiol to inhibit CD45, PTP1B, and CDC25. The effect of DTT on the activity of LGH00031 was studied. As shown in Figure 3A, LGH00031 inhibited CDC25B in a dose-dependent manner when 1 mmol/L DTT was added, whereas the inhibition caused by the compound disappeared when DTT was not included in the assay. DTT did not inhibit CDC25B activity without LGH00031 (data not shown). Another reducing thiol agent, dihydrolipoic acid, had a similar effect (Figure 3B). These results indicate that the action of LGH00031 *in vitro* depended on the presence of a reducing thiol agent such as

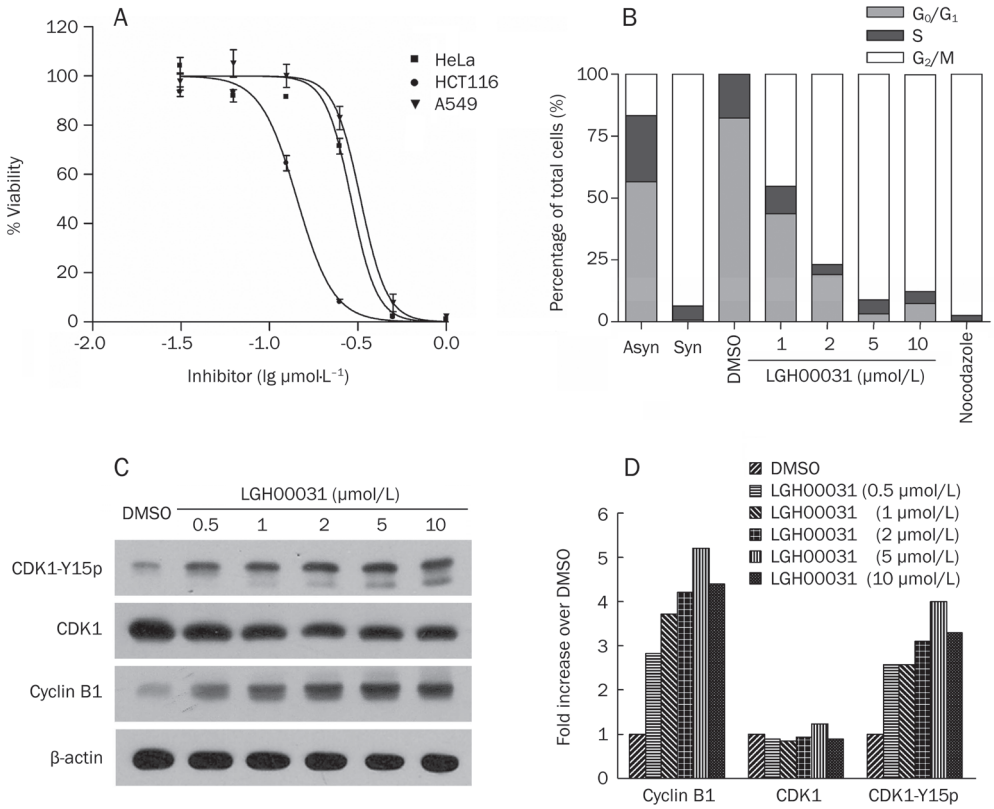

Figure 2. Cellular proliferation inhibition, cell cycle arrest, inhibition of CDK1 dephosphorylation caused by LGH00031. (A) The viability of three cancer cell lines after treated with indicated concentrations of LGH00031 for 3 days. (B) LGH00031 causes G_2/M phase arrest on HeLa cells. Asynchronous Cells (Asyn) were synchronized at G_2/M phase (Syn), and then treated with LGH00031 and 0.333 μmol/L nocodazole. Cells that treated with 1% DMSO was as a negative control. Cells were then harvested and subjected to flow cytometry analysis of their DNA content after propidium iodide staining. (C) LHG00031 inhibits CDK1 tyrosine 15 dephosphorylation and delays entry into mitosis. Cells in G_2/M phase were treated with indicated concentration of LGH00031 and DMSO for 4 h, and then harvested. Samples were processed for Western blot analysis. (D) The densitometric analysis of band intensity in Figure 2C is reported, using Quantity One software (Bio-Rad).

DTT or dihydrolipoic acid. To investigate further whether the inhibition by LGH00031 in the presence of DTT needs oxygen, the activity of LGH00031 against CDC25B was measured in the presence of 1 mmol/L DTT under both anaerobic and aerobic conditions. The anaerobic condition was created by conducting the experiment under nitrogen in oxygen-free buffer (see Materials and Methods for details). As shown in Figure 3C, LGH00031 inactivated CDC25B in a time-dependent manner under the aerobic condition. The activity of CDC25B was blocked completely by incubation with 0.144 μmol/L LGH00031 for 30 min in air. However, 90% of the CDC25B activity was maintained under the anaerobic condition.

The activity of LGH00031 against CDC25B *in vitro* depended on ROS generation

It has been reported that the para-quinonoid CDC25B inhibitors could irreversibly oxidize the cysteine present at the active site. To evaluate whether the ortho-quinonoid inhibitor CDC25B inhibits CDC25B by affecting the redox state, we measured the production of ROS in the assay with and without DTT or dihydrolipoic acid. As shown in Figure 4A and 4B, addition of LGH00031 induced the production of ROS in a dose-dependent manner in the presence of DTT or dihydrolipoic acid, whereas ROS production did not increase without DTT or dihydrolipoic acid. The results shown in Figures 3, 4A, and 4B indicate that the inhibition by LGH00031 of CDC25 was relative to the amount of ROS produced. We next asked whether the activity of LGH00031 is dependent on the generation of ROS and studied the relationship between ROS production and the activity of LGH00031. Different concentrations (U/mL) of superoxide dismutase (SOD) and catalase, which can reduce the production of ROS, were added to the assay and the level of ROS and the activity of LGH00031 were measured. The amount of ROS generated by incubation with LGH00031 declined markedly when SOD, catalase, or both were added to the assay (Figure 4C). The inhibition rate of LGH00031 against CDC25B also decreased in proportion to the decrease in ROS production (Figure 4D). These results indicate that the inhibition by LGH00031 was dependent on the generation of ROS.

LGH00031 inhibited cell proliferation and induced cell cycle arrest via ROS

To confirm whether the effect of LGH00031 on cells depends

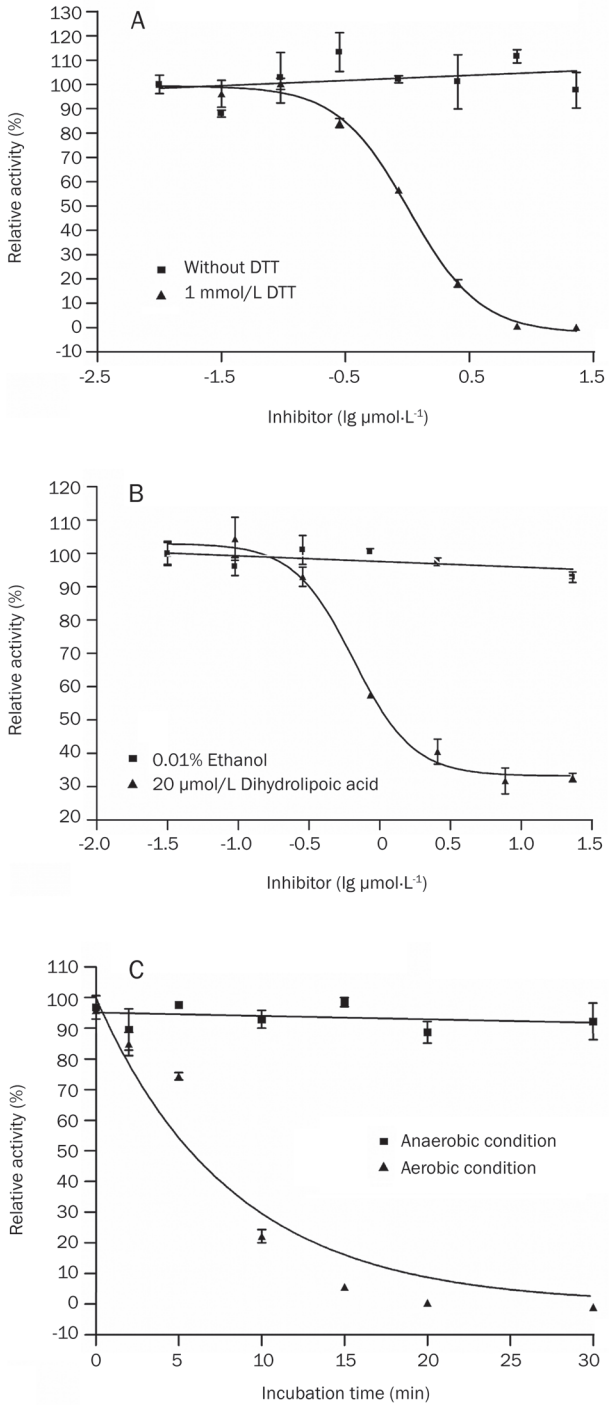

Figure 3. The inhibition by LGH00031 against CDC25B was mediated by DTT or dihydrolipoic acid and oxygen. (A) The inhibition by LGH00031 against CDC25B was dependent on the presence of DTT. (B) The inhibition by LGH00031 against CDC25B was dependent on the presence of dihydrolipoic acid. The residual activity of CDC25B was detected in the typical assay buffer with or without 1 mmol/L DTT, 20 μmol/L dihydrolipoic acid. (C) The inhibition by LGH00031 in the presence of DTT need oxygen. After incubated for indicated time in the absence or presence of oxygen, the residual activity of CDC25B was detected in typical assay buffer. Residual activity was the percentage of the activity of CDC25B in presence of LGH00031 relative to that in the absence of LGH00031 in the same condition.

on the amount of ROS generated, the ROS content was measured in cells treated with or without LGH00031 using the method mentioned above. Cellular ROS content increased in a dose-dependent manner after treatment with LGH00031 for 1 h. As shown in Figure 5A, the peak moved to the right with increasing LGH00031 concentration, and the percentage of cells in the defined field increased from 46% to 74% after treatment with 10 μmol/L LGH00031, indicating that LGH00031 increased the generation of cellular ROS.

The effects of ROS induced by LGH00031 on cell proliferation and the cell cycle were evaluated. NAC was used in the assay because it is a precursor of glutathione, which can decrease the content of ROS in cells. Cells were pretreated with NAC before LGH00031 treatment. As shown in Figure 5A, pretreatment with 20 μmol/L NAC for 30 min and then treatment with 2 μmol/L LGH00031 for 1 h decreased the percentage of cells with ROS from 56% to 10% compared with LGH00031-only treated cells. The relationship between ROS and the effects of LGH00031 were studied further. As shown in Figure 5B, pretreatment with NAC increased cell viability from 8.3% to 74.8% compared with LGH00031-only treated cells, indicating a nearly complete antagonism of the inhibitory effect of LGH00031 on cell proliferation. Accordingly, the G_2/M-phase cell cycle arrest was rescued from 81% to 49% (Figure 5C). Both the phosphorylation of CDK1 15 tyrosine and cyclin B1 protein decreased markedly (Figure 5D and 5E). All results indicated that the cellular activity of LGH00031 was impaired by NAC and that the inhibition of cellular CDC25B caused by LGH00031 was also dependent on the generation of ROS.

Discussion

The CDC25 phosphatases are considered potential targets for the development of new cancer therapeutic agents. The collective drug discovery efforts being directed toward identifying novel CDC25 inhibitors that work *in vitro* and that may even be active against human tumors *in viv*o have been reported[11, 19].

So far, only a few ortho-quinonoid CDC25 inhibitors have been reported. Coumpond 5169131, causing G_1/S and G_2/M arrest, and IC_{50} values against CDC25A, CDC25B, and CDC25C were reported as 5, 10.4, and 8.8 μmol/L[20]. KR61639 inhibits PTP1B (IC_{50}: 0.65 μmol/L) and CDC25B (IC_{50}: 0.67 μmol/L)[13], and cryptotanshinones and miltirone analogues are moderate inhibitors of CDC25B phosphatase (IC_{50}: 3.2–24 μmol/L)[16, 17]. The mechanism of action of these inhibitors is unclear. We found an IC_{50} of 0.97 μmol/L for the novel ortho-quinonoid CDC25B inhibitor LGH00031. We demonstrated that LGH00031 was an irreversible inhibitor of CDC25B with an apparent k_{obs}/I of 7579±647 $s^{-1}\cdot(mol/L)^{-1}$. We also investigated the inhibition by LGH00031 of the proliferation of cancer cell lines. As shown in Figure 2A, LGH00031 inhibited the proliferation of A549, HeLa, and HCT116 cells, with IC_{50} values of 0.143–0.328 μmol/L. All the traits mentioned above qualify LGH00031 as one of the most potent CDC25 inhibitors reported to date.

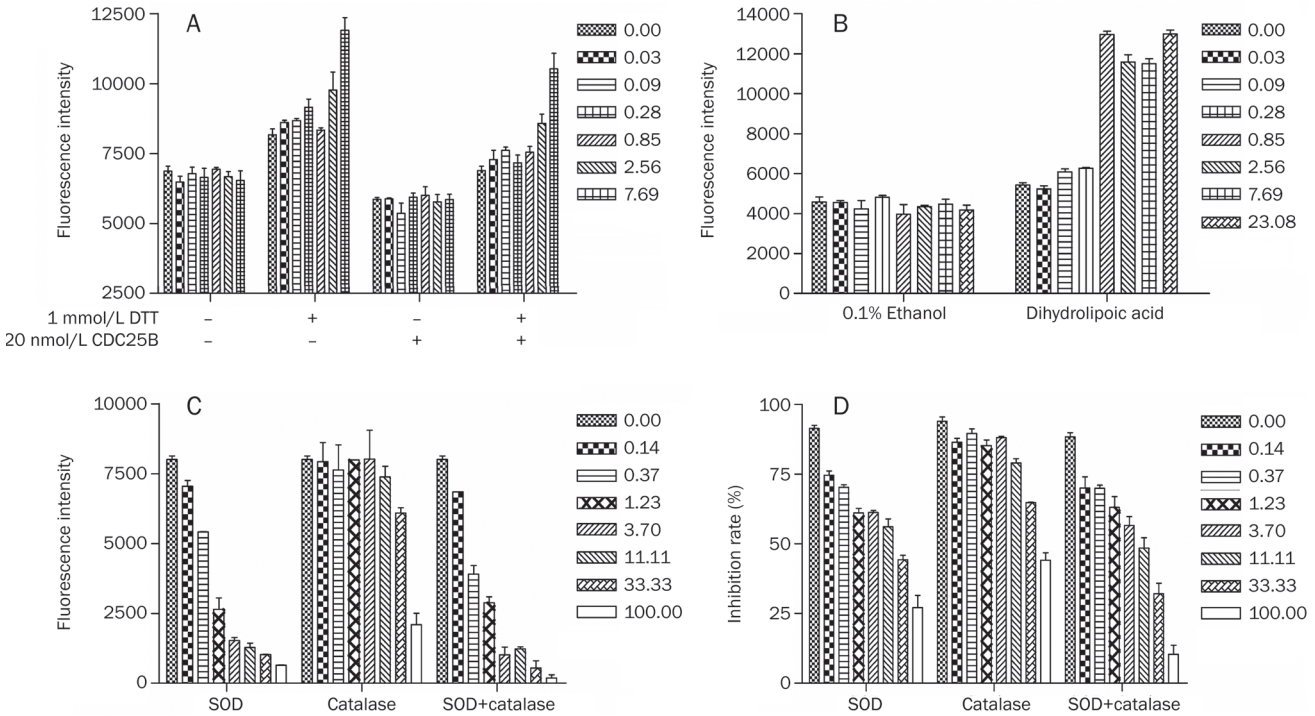

Figure 4. SOD and catalase reduced the activity of LGH00031 against CDC25B. (A) The production of ROS in the assay with or without DTT in the presence of different concentration of LGH00031. (B) The production of ROS in the assay with or without dihydrolipoic acid in the presence of different concentration of LGH00031. (C) The generation of ROS by LGH00031 in the presence of different concentration of SOD, catalase or both. The data shown in the figure was the value of the fluorescence intensity in the presence of 4.6 μmol/L LGH00031 minus that in the absence of LGH00031. (D) The inhibition rate of CDC25B caused by LGH00031 in the presence of different concentration of SOD, catalase or both. After 4.6 μmol/L LGH00031 incubated with different concentration SOD/catalase for 5 min, CDC25B activity was detected and the inhibition rate was the percentage of the activity of CDC25B in the absence of LGH00031 minus that in the presence of LGH00031 and SOD/catalase relative to that in the absence of LGH00031.

We also studied the effects of LGH00031 on other PTPases (Table 1) and found that LGH00031 had a better selectivity for CDC25s *in vitro* compared with JSP1, PTP1B, VHR, SHP1, CD45, and LAR. We evaluated the target specificity of LGH00031 at the cellular level. The CDC25B inhibitors blocked the cells at the G_2/M phase. Actually, we had evaluated the cell cycle arrest in asynchronous A549 cell line, which has G_2/M arrest potentiality (data not shown). Then HeLa cell, as the classical cell line for cell cycle evaluation was used to confirm the G_2/M arrest. Indeed, HeLa cells treated with LGH00031 were blocked at the G_2/M phase in a dose-dependent manner. The following evidence proves that LGH00031 is a superior CDC25B inhibitor in cultured cells. Tyrosine 15 phosphorylation of CDK1, a substrate of CDC25B, increased after LGH00031 treatment. Simultaneously, cyclin B1 accumulated in proportion to the dose of LGH00031, indicating that cells were prevented from entering mitosis by the inhibition of CDC25. Whereas, CDC25B and its serine 323 phosphorylation detected by Western blot did not change clearly even after treated for 12 h with 10 μmol/L LGH00031 (data not shown). Taken together, such evidence strongly supports the idea that the main cellular targets of LGH00031 are the CDC25 phosphatases.

Many of the most potent CDC25 phosphatase inhibitors reported to date are para-quinonoid-based compounds, such as the vitamin K3 analogues BN82685, NSC 663284, and IRC-083864[12, 15, 19, 21]. The mechanism of the inhibition caused by this kind of inhibitor suggests that these compounds act through the nucleophilic attack of electrophilic entities at a cysteine or at one of the vicinal serines, leading to the covalent modification of the enzyme or the irreversible oxidation of the cysteine present at the active site. To evaluate whether LGH00031 inhibits CDC25B by changing the redox state, we studied the effect of DTT on the inhibitory activity. In the absence of DTT, LGH00031 did not inhibit CDC25B and did not increase the ROS content. In contrast, the compound's activity was rescued by the addition of DTT, and the ROS level increased with an increasing dose of LGH00031 regardless of whether CDC25B was added (Figures 3A and 4A). In addition, the ROS-clearing reagents SOD and catalase reduced the magnitude of the inhibition by LGH00031 on CDC25B by reducing the generation of ROS (Figure 4C and 4D), confirming that its inhibitory activity on CDC25B *in vitro* is mediated, at least in part, by ROS production. This implies that the ortho-quinonoid CDC25 inhibitors inhibit CDC25B by increasing the generation of ROS, similar to the action of para-quinonoid compounds. Other studies have reported that the activities of ortho-quinonoid inhibitors against CD45 and

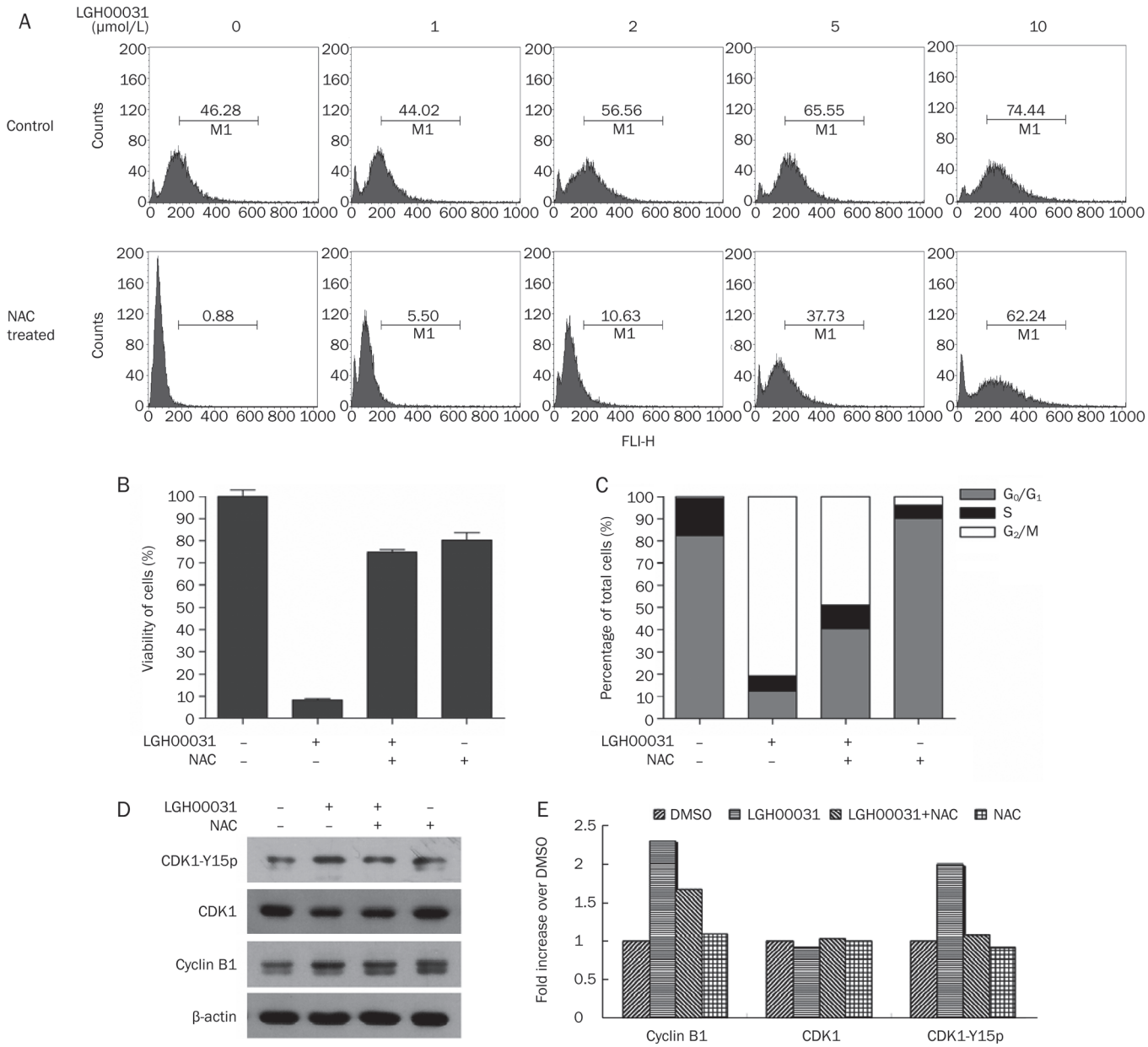

Figure 5. LGH00031 inhibited cell proliferation and induce cell cycle arrest via ROS. (A) LGH00031 increased the cellular ROS level. Cells were seeded into 6-well plate, and cultured over night. In the second day, cells were pre-incubated with 20 mmol/L NAC or untreated for 30 min. After treated with different concentration of LGH00031 for 1 h, cellular ROS was detected as the method described. (B) NAC reversed the inhibition of cell proliferation caused by 2 μmol/L LGH00031 treatment. (C) NAC rescued the G_2/M cell cycle arrest caused by LGH00031. (D) Pretreated with NAC, the inhibition of dephosphorylation of CDK1 and the accumulation of cyclin B1 caused by LGH00031 was impaired. (E) The densitometric analysis of band intensity in Figure 5D is reported, using Quantity One software (Bio-Rad).

PTPα are mediated by ROS derived from oxygen and the DTT-dependent redox cycle[22, 23].

However, there is no clear evidence that the ROS generated by inactivation of quinone-catalyzed PTP affects cell proliferation and the cell cycle. LGH00031 increased the levels of ROS in HeLa cells, an effect similar to that of DA3003-1 and JUN1111[15]. The effect of ROS on cell proliferation was evaluated with NAC, a precursor of glutathione. As shown in Figure 5A, NAC decreased the generation of ROS induced by 2 μmol/L LGH00031 from 56% to 10%. Correspondingly, the cell viability increased from 8.3% to 74.8%, and the percentage of cells at the G_2/M phase decreased from 81% to 49% (Figure 5B and 5C), hinting at the pivotal role of ROS in mediating the effects of LGH00031 on cell proliferation and the cell cycle. The cyclin B1 level and dephosphorylation of CDK1 tyrosine 15 were also rescued from the inhibition of LGH00031 by the addition of NAC (Figure 5D and 5E), also suggesting that the inhibition of cellular CDC25B caused by LGH00031 is medi-

ated by ROS. With regard to the specificity of LGH00031, Contour-Galcera *et al* commented that the unusually low pK_a of the active-site cysteine in CDC25 makes it highly susceptible to reactions with ROS. On the other hand, LGH00031 might interact with CDC25B, which could increase the ROS concentration around CDC25B further and make it highly specific for CDC25.

It has been reported that the redox cycle of quinone-catalyzed PTP inactivation is not initiated between the compound and PTP but relies on another molecule, such as DTT[22, 23], although the identity of this molecule in the cell is unclear. Hydrolipoic acid can act as both a free radical scavenger and a radical generator[24]. Similar to other vicinal thiols, dihydrolipoic acid (reduced lipoic acid) is oxidized more easily than are monothiols, leading to the high activity in the -SH/-S-S- interchange reactions. The observation of the thiyl radical and ROS derived from dihydrolipoic acid suggests that this compound may act as a pro-oxidant under the right conditions. As our results shown in Figures 3B and 4B, the activity of LGH00031 against CDC25B was rescued by the addition of 20 μmol/L dihydrolipoic acid to the DTT-free assay buffer. At the same time, ROS were generated in a dose-dependent manner (Figure 4B). Our results demonstrate that LGH00031 inhibits the activity of CDC25B through dihydrolipoic acid, and, like DTT, LGH00031 has a high tendency to generate ROS. This implies that DTT can be replaced with a high concentration of dihydrolipoic acid to take part in the redox cycle of LGH00031 in cell However, this suggestion does not exclude the possibility that other molecules could catalyze LGH00031 in cell or that other quinonoid PTP inhibitors also produce ROS, thereby changing the cellular redox state and the activity of PTP. Our data support the observation that the irreversible inhibition of CDC25B by LGH00031 is dependent on oxygen and DTT or dihydrolipoic acid. Based on both biochemical and cellular data, we propose that the ROS generated rather than the direct interaction with CDC25B plays a key role in the inactivation of CDC25B by LGH00031 (Figure 6).

In summary, an irreversible ortho-quinonoid inhibitor of CDC25B, LGH00031, was reported. The activity of this inhibitor of CDC25 *in vitro* and the strong effects against cancer cells suggest that it is one of the most potent CDC25 inhibitors published to date. Its activity against CDC25B *in vitro* was mediated by ROS derived from oxygen and DTT. And the pivotal role of ROS in the inhibition by LGH00031 on cell proliferation, the cell cycle, and the inactivation of cellular CDC25B were identified. At last, dihydrolipoic acid is proposed as the initiator of ROS in cells treated with LGH00031.

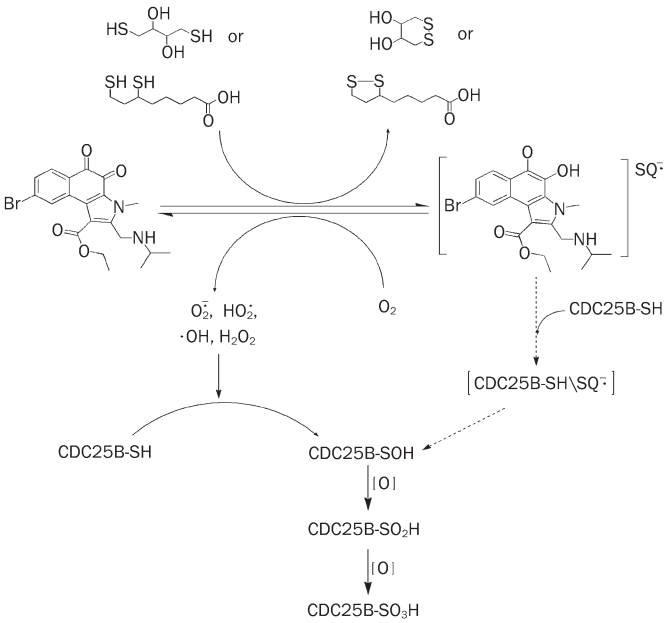

Figure 6. Proposed scheme for the catalytic inactivation of CDC25B by LGH00031 through redox cycling. In the presence of DTT *in vitro* and possibly dihydrolipoic acid in cell, LGH00031 rapidly undergo reduction to the corresponding semiquinone anion radicals ($RQ^{\cdot-}$). The produced ROS catalyzes the step by step oxidation of the active site cysteine of CDC25B to the sulfonic acid.

Acknowledgements

This work was supported by National Natural Science Foundation of China (30801405); Major State Hi-tech Research and Development Program Grant (2006AA02Z315); and Qi Ming Xing Foundation of Shanghai Ministry of Science and Technology (08QH14005).

Author contribution

Prof Jia LI designed research; Xu FENG, Li-na WANG, Jun-qing DU, Yue-yang ZHOU, Hai-ping YU, and Yu-bo ZHOU performed research; Yu-bo ZHOU, Yi ZANG, and Jing-ya LI analyzed data; Yu-bo ZHOU, Xu FENG, and Prof Jia LI wrote the paper.

References

1 Rudolph J. Cdc25 phosphatases: structure, specificity, and mechanism. Biochemistry 2007; 46: 3595–604.
2 Xing X, Chen J, Chen M. Expression of CDC25 phosphatases in human gastric cancer. Dig Dis Sci 2007; 53: 949–53.
3 Sasaki H, Yukiue H, Kobayashi Y, Tanahashi M, Moriyama S, Nakashima Y, *et al*. Expression of the cdc25B gene as a prognosis marker in non-small cell lung cancer. Cancer Lett 2001; 173: 187–92.
4 Ngan ES, Hashimoto Y, Ma ZQ, Tsai MJ, Tsai SY. Overexpression of Cdc25B, an androgen receptor coactivator, in prostate cancer. Oncogene 2003; 22: 734–9.
5 Cangi MG, Cukor B, Soung P, Signoretti S, Moreira G Jr, Ranashinge M, *et al*. Role of the Cdc25A phosphatase in human breast cancer. J Clin Invest 2000; 106: 753–61.
6 Galaktionov K, Lee AK, Eckstein J, Draetta G, Meckler J, Loda M, *et al*. CDC25 phosphatases as potential human oncogenes. Science 1995; 269: 1575–7.
7 Yao Y, Slosberg ED, Wang L, Hibshoosh H, Zhang YJ, Xing WQ, *et al*. Increased susceptibility to carcinogen-induced mammary tumors in MMTV-Cdc25B transgenic mice. Oncogene 1999; 18: 5159–66.
8 Ma ZQ, Chua SS, DeMayo FJ, Tsai SY. Induction of mammary gland

hyperplasia in transgenic mice over-expressing human Cdc25B. Oncogene 1999; 18: 4564–76.
9 Lammer C, Wagerer S, Saffrich R, Mertens D, Ansorge W, Hoffmann I. The cdc25B phosphatase is essential for the G_2/M phase transition in human cells. J Cell Sci 1998; 111 (Pt 16): 2445–53.
10 Xu X, Yamamoto H, Liu G, Ito Y, Ngan CY, Kondo M, *et al*. CDC25A inhibition suppresses the growth and invasion of human hepatocellular carcinoma cells. Int J Mol Med 2008; 21: 145–52.
11 Contour-Galcera MO, Sidhu A, Prevost G, Bigg D, Ducommun B. What's new on CDC25 phosphatase inhibitors. Pharmacol Ther 2007; 115: 1–12.
12 Shimazawa R, Suzuki T, Dodo K, Shirai R. Design and synthesis of dysidiolide analogs from vitamin D3: novel class of Cdc25A inhibitors. Bioorg Med Chem Lett 2004; 14: 3291–4.
13 Cheon HG, Kim SM, Yang SD, Ha JD, Choi JK. Discovery of a novel protein tyrosine phosphatase-1B inhibitor, KR61639: potential development as an antihyperglycemic agent. Eur J Pharmacol 2004; 485: 333–9.
14 Kar S, Wang M, Yao W, Michejda CJ, Carr BI. PM-20, a novel inhibitor of Cdc25A, induces extracellular signal-regulated kinase 1/2 phosphorylation and inhibits hepatocellular carcinoma growth *in vitro* and *in vivo*. Mol Cancer Ther 2006; 5: 1511–9.
15 Brisson M, Nguyen T, Wipf P, Joo B, Day BW, Skoko JS, *et al*. Redox regulation of Cdc25B by cell-active quinolinediones. Mol Pharmacol 2005; 68: 1810–20.
16 Huang WG, Jiang YY, Li Q, Li J, Li JY, Lu W, *et al*. Synthesis and biological evaluation of (G)-cryptotanshinone and its simplified analogues as potent CDC25 inhibitors. Tetrahedron 2005; 61: 1863–70.
17 Huang W, Li J, Zhang W, Zhou Y, Xie C, Luo Y, *et al*. Synthesis of miltirone analogues as inhibitors of Cdc25 phosphatases. Bioorg Med Chem Lett 2006; 16: 1905–8.
18 Feng X, Wang LN, Zhou YY, Yu HP, Shen Q, Zang Y, *et al*. Discovery and characterization of a novel inhibitor of CDC25B, LGH00045. Acta Pharmacol Sin 2008; 29: 1268–74.
19 Brezak MC, Quaranta M, Contour-Galcera MO, Lavergne O, Mondesert O, Auvray P, *et al*. Inhibition of human tumor cell growth *in vivo* by an orally bioavailable inhibitor of CDC25 phosphatases. Mol Cancer Ther 2005; 4: 1378–87.
20 Brisson M, Nguyen T, Vogt A, Yalowich J, Giorgianni A, Tobi D, *et al*. Discovery and characterization of novel small molecule inhibitors of human Cdc25B dual specificity phosphatase. Mol Pharmacol 2004; 66: 824–33.
21 Brezak MC, Valette A, Quaranta M, Contour-Galcera MO, Jullien D, Lavergne O, *et al*. IRC-083864, a novel bis quinone inhibitor of CDC25 phosphatases active against human cancer cells. Int J Cancer 2009; 124: 1449–56.
22 Wang Q, Dube D, Friesen RW, LeRiche TG, Bateman KP, Trimble L, *et al*. Catalytic inactivation of protein tyrosine phosphatase CD45 and protein tyrosine phosphatase 1B by polyaromatic quinones. Biochemistry 2004; 43: 4294–303.
23 Bova MP, Mattson MN, Vasile S, Tam D, Holsinger L, Bremer M, *et al*. The oxidative mechanism of action of ortho-quinone inhibitors of protein-tyrosine phosphatase alpha is mediated by hydrogen peroxide. Arch Biochem Biophys 2004; 429: 30–41.
24 Mottley C, Mason RP. Sulfur-centered radical formation from the antioxidant dihydrolipoic acid. J Biol Chem 2001; 276: 42677–83.